

Microstructural Characterization of the Infarct Border Zone in Humans with In Vivo Diffusion Tensor MRI and “Gray-Zone” Late Gadolinium Enhancement

Choukri Mekkaoui¹, Christian T Stoeck², Marcel P Jackowski³, Timothy G Reese⁴, Sebastian Kozerke⁵, and David E Sosnovik⁶

¹Harvard Medical School - Massachusetts General Hospital, Boston, MA, United States, ²University and ETH Zurich, Zurich, Switzerland, ³University of São Paulo, São Paulo, Brazil, ⁴Athinoula A Martinos center for Biomedical imaging, Boston, United States, ⁵University and ETH Zurich, Zurich, Switzerland, ⁶Harvard Medical School - Massachusetts General Hospital, Boston, United States

Target Audience: Scientists/clinicians interested in MRI of the myocardium.

Purpose: The area of myocardium adjacent to an infarct (border zone) plays a major role in the development of mechanical and electrical dysfunction as the heart remodels. Intermediate signal on late gadolinium enhancement (LGE) has been used to delineate the infarct periphery and border zone.¹ However, the microstructural properties of the border zone in the human heart in vivo have not yet been characterized. Here we used in vivo diffusion tensor MRI (DTI) and LGE in patients with recent myocardial infarctions to elucidate the microstructural properties of the infarct border zone.

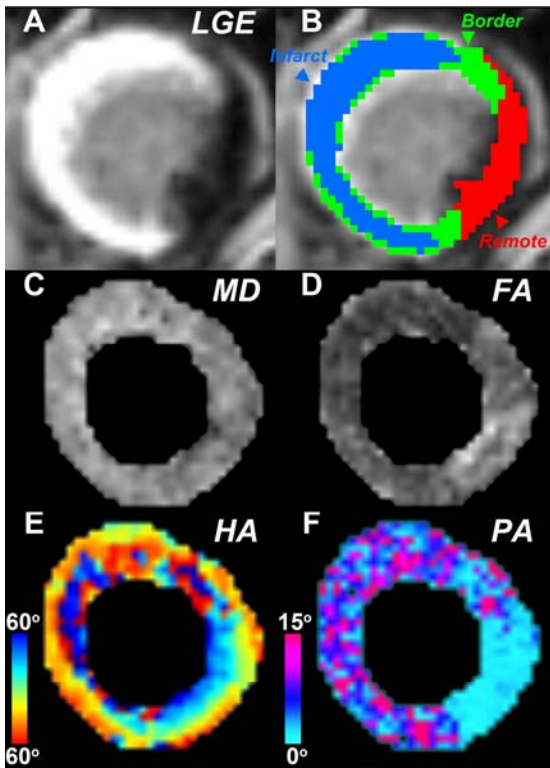


Figure 1: (A) Short axis LGE image in a patient with a recent myocardial infarction. (B) Segmentation of the LGE image into remote (red), infarct (blue), and border (green) zones. (C, D) Mean diffusivity (MD) in the border zone is increased and fractional anisotropy (FA) is decreased. (E, F) The transmural distribution of fiber helix angles (HA) in the border zone is abnormal and the propagation angle (PA) is increased.

DISCUSSION: Late gadolinium enhancement (LGE) is increasingly being used to define “gray zones” in infarcted myocardium. Here for the first time we define the microstructural properties of the border zone in vivo using DTI and LGE. We show that an increase in LGE in the border zone of just 1 standard deviation above normal is associated with significant microstructural abnormality. The border zone is significantly less anisotropic than normal myocardium and is highly heterogeneous, containing both regions of coherent and incoherent myofiber tracts. In addition, the orientation of the fiber tracts present is highly abnormal, which likely contributes to the progressive loss of function in the border zone.

Conclusion: The border zone has a highly complex and heterogeneous microstructure that can be resolved with in vivo DTI. This could play an important role in clinical care, where knowledge of the specific microstructure of the border zone could be of major value.

Methods: Patients with acute myocardial infarction (MI, n=3) were scanned prior to discharge on a clinical 1.5T scanner with a diffusion-encoded stimulated echo EPI sequence and the following parameters: resolution 1.75x1.75x8 mm³, b-value of 500 s/mm², 6 diffusion encoding directions and 8 averages. Imaging was performed in the diastolic sweet spot of the cardiac cycle to mitigate the effect of strain. Late gadolinium enhancement (LGE) was performed after the injection of 0.2 mmol/kg of Gd-DTPA using an inversion recovery gradient echo sequence. Infarcted myocardium by LGE was defined by a signal intensity > 2 standard deviations (SD) above normal myocardium.¹ The infarct was further subdivided into the infarct core (>3 SD above normal) and the infarct periphery (2-3 SD above normal).¹ The border zone was defined by signal between 1-2 SD above normal. The diffusion tensor field was determined and diagonalized to yield the principal (e_1/λ_1), secondary (e_2/λ_2), and tertiary (e_3/λ_3) eigenvectors/values. Mean diffusivity (MD), fractional anisotropy (FA), helix angle (HA), and propagation angle (PA) were calculated as previously described.²⁻⁴ In addition, HA variance at several transmural depths was measured. Fiber tracts were constructed by integrating the primary eigenvector field into streamlines using a 5th order adaptive Runge-Kutta approach and color coded by HA. Values in the infarct, border, and remote zones were compared using ANOVA.

Results: A total of 16 short axis LGE images were segmented and analyzed. A representative LGE image before and after segmentation is shown in Figure 1A-B. MD, FA, HA, and PA maps at the corresponding slice location are shown in Figures 1C-F. MD, PA, and HA variance in the border zone were significantly higher than that of normal myocardium but also lower than in the infarct zone. Likewise, FA in the border zone was lower than that of normal myocardium but higher than in the infarct. Average values are plotted in Figure 2A-D. Fiber architecture in the remote zone showed the characteristic crossing helical pattern of subendocardial (blue) and subepicardial (yellow-red) fibers (Fig. 2E). Fiber architecture in the border zone was markedly perturbed and heterogeneous (Fig. 2F). While coherent tracts could be resolved in some portions of the border zone, large gaps with no coherent fiber tracts were seen. In addition, the orientation of the tracts in the subendocardium and subepicardium was similar and the characteristic crossing helical pattern was lost. Severe microstructural disarray was seen in the infarct zone with the near complete loss of normal fiber orientation (Fig. 2G).

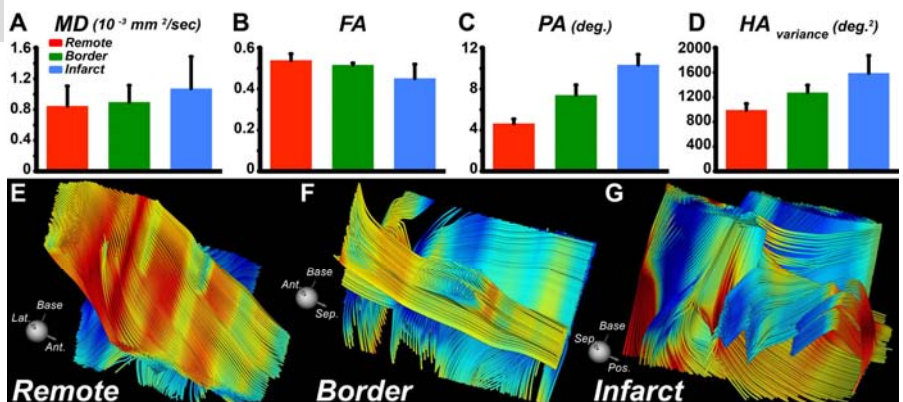


Figure 2: (A-D) Plots of MD, FA, PA, and HA variance in the remote, border, and infarct zones. A clear difference in all indices is seen between the remote myocardium and both the infarct and border zones. (E-G) Fiber tracts colored by HA. (E) In the remote zone, the fiber tracts are dense and coherent. The subepicardial (yellow-red) and subendocardial (blue) fibers cross over each other at an angle of approximately 120°. (F) The border zone is highly heterogeneous. Some areas of tract coherence are seen but large gaps are also present. The remaining fibers have lost the characteristic crossing helical orientation. (G) Severe disarray is seen in the infarct zone.

References: 1) Yan AT *et al.* Circulation 2006. 2) Mekkaoui C *et al.* ISMRM 2011. 3) Mekkaoui C *et al.* JCMR 2012. 4) Mekkaoui C *et al.* JCMR 2013.